Assessment of biogeochemical trends in soil organic matter sequestration in mountain Mediterranean calcimorphic soils (Almería, Southern Spain)

Isabel Miralles [a], Raúl Ortega [b], Manuel Sánchez-Marañón [a], Miguel Soriano [b], Gonzalo Almendros [c,*]

[a] *Dpto. Edafología y Química Agrícola. Facultad de Farmacia. Universidad de Granada. Campus La Cartuja s/n. 18071-Granada, Spain*
[b] *Dpto. Edafología y Química Agrícola. Facultad de Ciencias Experimentales. Universidad de Almería. Escuela Politécnica Superior, 04120-Almería, Spain*
[c] *Centro de Ciencias Medioambientales (CSIC), Serrano 115 B, 28006-Madrid, Spain*

Abstract

Total soil organic matter levels and humic acid formation processes in mountain calcimorphic soils from Sierra María-Los Vélez Natural Park (Almería, Southern Spain) were found to differ depending on soil use (pine and oak forests, and cleared areas either cultivated or affected by bush encroachment). Biogeochemical indicators such as the concentration of exchangeable cations, or of the concentration of the different types of humic substances were neither influenced by the type of vegetation nor soil use. In fact, multidimensional scaling and multiple correlations suggest that soil carbon sequestration processes are controlled by small-scale topographical features and their impact on water holding capacity. From a qualitative viewpoint, there were two more or less-defined sets of soils: one set consisted of humic acids with marked aliphatic character, displayed intense 2920 cm^{-1}, and had low optical density. The resolution-enhanced infrared spectra suggested typical lignin patterns and well-defined amide bands, which point to a selective preservation of comparatively young organic matter. This situation contrasts with that in other set of soils with low C levels (<20 g kg^{-1}) where humic acids with featureless IR spectra showed high aromaticity and were associated to perylenequinonic chromophors

* Corresponding author. Tel.: +34-91-7452500, ext 220; fax +34-91-5640800; *E-mail address:* humus@ccma.csic.es (G. Almendros)

of fungal origin: this is considered the consequence of overlapping biogeochemical mechanisms involving both microbial synthesis and condensation processes. The results from visible and infrared derivative spectroscopies suggest that the reliability of statistically assessing the biogeochemical performance of the different uses on the site studied in terms of the intensity of the prevailing humic acid formation mechanisms, i.e., accumulation of inherited macromolecular substances in the former set, vs. microbial synthesis including the condensation of precursors of low molecular weight substances in the latter.

Keywords: Humic acid, Humic substances, Humus fractions, Humification pathways, Fungal melanins, Perylenequinones, Lignin alteration, Visible spectroscopy, Infrared spectroscopy

1. Introduction

Environmental factors influencing soil mechanisms responsible for C stabilization are still not very well known (Kögel-Knabner et al., 2005). The knowledge of such processes is especially relevant as regards to the justification of different levels of resilience. In particular some, calcimorphic soils may display peculiar features associated with encapsulation processes of particulate organic matter fractions which favour the molecular preservation of plant inherited materials (Derenne and Knicker, 2000) as well as the early immobilization of soluble precursors of humic macromolecules (Duchaufour et al., 1975). Apart from this, the buffering effect of carbonates in most soil microcompartments may lead to balance the effect of vegetation (e.g., in conifer forests,

which frequently led to acid humus types) which may also play a role in limiting the solubility of most macro- and microelements in soil. Mainly in semiarid Mediterranean areas, these facts may result in soil formations in which characteristics are unrelated to types of vegetation, making it also difficult the assessment of environmental impacts (Oyonarte et al., 1994).

At this point, the Sierra María-Los Vélez Natural Park (Almería, Southern Spain) could behave as model scenario for C cycling processes in virgin and cultivated calcimorphic sites from Continental Mediterranean areas. This site displays large phytosociological variability ranging from Mediterranean sclerophyllic forest to ancient conifer forests. In the course of the last fifty years this region has suffered dramatic disturbance either leading to cleared sites subjected to bush encroachment or to areas for continuous agricultural crops.

The prevailing limestone substrate in this Natural Park, has been considered to play a role in the comparatively similar properties of the humus formations irrespectively of their local use and management (Oyonarte et al., 1994). Nevertheless, it could be expected that the diversity generated by elevation and slope at this mountain site—and the derived effects of climatic gradient and potential erosion—would play an additional role in soil formation processes.

The present study tackles with a methodological assessment of environmental impact, based on a spectroscopic monitoring of the fate of the major biomass constituents incorporated in the soil, and the formation processes of humic substances. From the biogeochemical viewpoint, the experimental design could also be considered suitable to unravel factors affecting soil C sequestration in the different soils.

2. Materials and methods

2.1. Sampling sites

The Natural Park Sierra María-Los Vélez (Fig. 1) is located in the outermost Northern sector of the province of Almería (Southeastern Spain), and lies in the Eastern sector of the Baetica Mountain system (Egea, 1986). The geologic substrate (Table 1) consists of sedimentary rocks (limestones, marls and dolomites). The landscape in the forest sites consists of mountain ranges and valleys, the altitudinal range being between 800 and 2045 m.a.s.l. The climate is of the Mediterranean-type with strong continental features, ranging from the semiarid to sub-humid kind , which implies mild temperatures (between 11.9 and 16.9 ºC), unreliable and torrential precipitations with equinoctial maxima and one summer dry season. The topography of the area, in addition to climatic, soil and lithologic diversities, defines toposequential bioclimatic areas i.e.,: i) Oromediterranean, dominated by *Pinus nigra* Arn, subsp. *salzmannii*, ii) Supramediterranean, with *Quercus ilex* L. subsp. *rotundifolia* and re-afforested *Pinus halepensis* Mill., and iii) Mesomediterranean, where communities with secondary *Thymus* sp. and *Rosmarinus* sp. brushlands coexist with almond trees and cereal crops (Cueto and Blanca, 1997).

The dominant vegetation series in the whole Park is *Bupleuro-Querceto rotundifoliae,* which occupies the Mesomediterranean bioclimatic step excepting the Southern and Eastern sides of the Sierra María, where *Paeonio-Querceto rotundifoliae* predominates. The Supramediterranean step shows characteristic vegetation belonging to the *Berberido-Querceto rotundifoliae* series, excepting the most humid spots with *Daphno-Acereto granatensis* as the dominant formation. The remaining Supramediterranean step corresponds to the *Junipero thuriferae-Querceto rotundifoliae* series. Finally, the alpine brush in the Oromediterranean step of the Sierra María consists

106 of relictual plant communities belonging to the *Daphno-Pineto sylvestris* series (Rivas
107 Martínez, 1987). The soil types are mainly Mollic-Petric Calcisols, Rendzic Leptosols,
108 Hypocalcic Calcisols and Hypercalcic Calcisols, Luvic Calcisols and Petric Calcisols
109 (Table 1).
110
111 *2.2. Topographical and geomorphological features*
112
113 Field data were taken during sampling campaigns or calculated with a Geographical
114 Information System Arc GIS 8.1 and Solar Analyst 1.0. derived from a Digital Terrain
115 Model with a resolution of 20 m (Miralles et al., 2002). The variables obtained and
116 processed (Moore et al., 1991) were i) the wetness index, ii) the slope length factor i.e, a
117 measure of the potential for sediment transportation, iii) the contributing area, iv) the plan
118 curvature i.e., curvature transverse to the slope or contour curvature, which is related to the
119 converging/diverging flow and soil water content, v) the slope profile curvature, related to
120 flow acceleration, which is an important determinant of erosion and deposition processes on
121 the hill slope scale, vi) the global solar radiation at summer solstice, vii) the global solar
122 radiation at winter solstice, viii) the global solar radiation at equinox, ix) the hours of
123 insolation at summer solstice, x) the hours of insolation at winter solstice, and xi) the hours
124 of insolation at equinox.
125
126 *2.3. General analytical procedures*
127 After litter removal, soil samples (around 500 g) were collected with a spade. The
128 samples (obtained by mixing three subsamples about 20 m apart in the field) were taken
129 from the 10 uppermost cm of the soil profile. In the laboratory, the air-dried soil samples
130 were homogenised to 2 mm (fine earth) with a wooden cylinder. A series of colour

parameters, *i.e.*, CIELAB L^*, C_{ab}^*, H_{ab} (CIE, 1986) were calculated from soil reflectance spectra (360–740 nm) obtained with a Minolta CM-2600d spectrophotometer (d/8 geometry) operating with the specular component excluded, illuminate D65, and observer 10º. Soil bulk density was measured using a cylindrical core of known volume, and particle density was measured with a pycnometer. The granulometric analysis was carried out following Soil Conservation Service (1984). Soil water repellence (Savage et al., 1972) was estimated by the water drop penetration time (WDPT). Soil pH was measured in a 1:1 soil:water suspension. Total carbonates were measured as $CaCO_3$ with the Bernard calcimeter (CSIC, 1969). The soil water holding capacity was determined at -1500 kPa in a pressure-membrane extractor (Richards, 1954). Exchangeable elements were extracted with 1 mol l^{-1} NH_4Ac at pH 7 (Soil Conservation Service, 1984). Potassium was determined by flame ionization spectroscopy, whereas calcium and magnesium were measured by atomic absorption spectroscopy. Free iron was colorimetrically determined after dithionite-citrate extraction (Holgrem, 1967). Total nitrogen was determined by micro-Kjeldahl digestion and soil carbon by wet oxidation using dichromate in acid medium followed by redox titration (Nelson and Sommers, 1982).

2.4. Soil humus fractions

The methods applied for the isolation and quantitative determination of the humus fractions were based on standard procedures (Duchaufour et al., 1975; Dabin, 1971). The separation of the particulate, low density fraction with the not-yet decomposed organic particles was carried out with soil sample 10 g suspended in 2 mol l^{-1} H_3PO_4. After rotary stirring for 1 min, the floating light soil fraction consisting of free organic matter was isolated by centrifuging the suspension, washed with distilled water and analyzed for total C.

156 The yellow-coloured supernatant solution resulting from the density fractionation, and
157 containing the organic matter dissolved in the H_3PO_4 solution was stored for further analysis.
158 This fraction was labeled as the H_3PO_4-fulvic fraction, and considered a fulvic fraction less
159 strongly associated with the soil matrix than the corresponding fulvic acid removed with the
160 NaOH treatments used to extract soil humic acids described below.

161 The soil residue remaining after centrifugation was shaken with 0.1 mol l^{-1} $Na_4P_2O_7$
162 followed by 0.1 mol l^{-1} NaOH (horizontal motion mechanical shaking for 3 h) and
163 centrifuged. This treatment was repeated up to 5 times, the dark brown extract obtained
164 corresponding to the *total humic extract* (humic acid + fulvic acid). Two aliquots were taken
165 from this extract, and precipitated with H_2SO_4 (1:1 by vol.) for further determination of the
166 amounts of the acid-soluble fulvic acid and the precipitated humic acid fraction,
167 respectively.

168 The soil residue after the alkaline extraction was washed with distilled water and
169 desiccated at 50 ºC. The C concentration in this residue was total humin.

170

171 *2.5. Preparative isolation and purification of the humic acids*

172

173 For de-ashing, the humic acid fraction was concentrated by precipitating the total
174 humic extract with 6 mol l^{-1} HCl to pH=2, redissolved in 0.5 mol l^{-1} NaOH and centrifuged
175 at 43500 *g*. After discarding the insoluble residue (particulate soil organic and mineral
176 fractions) the dark brown surnatant solution with the sodium humate was reprecipitated by
177 adding HCl and the resulting gel was dialysed against distilled water in cellophane bags
178 (Visking dialysis tubing**,** molecular weight cutoff 12000–14000; pore diameter ca. 25 Å**,**
179 Medicell) and desiccated at 40ºC. Complete quantitative fractionation of soil organic matter
180 into free organic matter, humic acid and fulvic acid (H_3PO_4), was carried out only in

selected samples because these classical variables were assumed not to be very informative on the humification pathways, where humic acid quality is more important than humic acid quantity. In the whole set of samples the total amount of humic acid (in C) were determined in addition to the spectroscopic indicators as described in the following.

2.6. Spectroscopic characterization of the humic acids

In order to determine the optical density, which is considered an index of the aromaticity of humic substances (Traina et al., 1990), humic acid solutions of 66.6 mg l^{-1} C in 0.02 mol l^{-1} NaOH were prepared. The second-derivative visible spectra were obtained from the above solutions using a Shimadzu UV-240 spectrophotometer, OPI-2. For infrared spectroscopy a Shimadzu FTIR-8400 PC was used. To obtain a second set of resolution-enhanced spectra, the digitised spectra were processed by an algorithm consisting of subtracting the original spectrum from a multiple of its 2nd derivative, then applying a moving averages smoothing algorithm (Rosenfeld and Kak, 1982; Almendros and Sanz, 1992).

2.7. Data treatments

Statistical data treatments, mainly simple and multiple regression analyses, variance analysis, principal components and factorial discriminant analysis, cluster analysis and multidimensional scaling, were carried out by the STAT-ITCF software (ITCF, 1988) and the programs by Orlóci and Kenkel (1985). In the case of nonlinear mapping treatments standardized variable sets were used.

208 **3. Results**

209 *3.1. General analytical characteristics*

210

211 The analysis of the topographical variables (Table 2) suggested mosaic-like spatial
212 distribution patterns, which overlapped with an ill-defined altitudinal gradient in specific
213 transects. In general the wetness index (Table 2) is high, indicating several spots with low
214 drainage where water accumulates frequently coinciding with the lower slope. About 46%
215 of the total surface shows a slope length factor (SLF) higher than 20, and ca. 31% shows
216 values of between 5 and 10. This suggests a large potential for sediment transportation and
217 consequently important water erosion, mainly in steep slope areas.

218 Table 3 shows the main analytical characteristics of the topsoil. In general, the
219 amount of carbonates in soils developed under a limestone substrate (ranging from
220 between 5 to 940 g kg^{-1}) which indicates a variable decarbonation of the calcic substrate.
221 Soil organic C ranged from between 195 to 6 g kg^{-1} as it could be expected from the
222 differences between ancient forest soils and cleared sites. In agreement with other authors
223 (Schulze et al., 1993; Spielvogel et al., 2004), soil lightness L^* decreased as the carbon
224 content increased (Fig. 2). This relationship, however, was curvilinear since soils with a
225 high C content from the upper areas of the altitudinal gradient (mainly ancient forest),
226 displayed an L^* value similar to those from cleared or recently reafforested soils having a
227 comparatively low amount of organic matter. This soil colour index could be pointing to
228 variying organic matter quality in the different soils as it will be discussed in the
229 following.

230

231

232

3.2. Soil humus fractions

Table 4 shows the absolute concentration of the different forms of organic C in the soil, whereas the values in Fig. 3 are calculated as percentages of the total C, and samples were classified in terms of elevation at the sampling sites irrespective of the types of vegetation. The almost complete transformation of plant residues after their incorporation in the soil is shown by the low values of the light fraction. Concerning the colloidal fractions, the soils show comparatively high levels of fulvic acids either directly extracted from soil with an acid pH (humic acid to fulvic acid ratios <1) or separated from the total humic extract. This fact, as well as the relatively high amounts of humin, could be caused by the physical retention of particulate fractions and the insolubilising effect on soluble fractions, both expected from the calcic substrate (Duchaufour, 1977).

3.3. Spectroscopic studies: Visible spectroscopy

The visible spectra of humic acids showed monotonous spectra, although the specific extinctions varied from between 0.3 and 1.2 (E_4, Table 5). Humic acid solutions showed high optical densities; during measurements, and to comply with the Lambert-Beer's law, the spectra were acquired from solutions diluted up to three times as regards the standard concentration proposed by Kononova (1961). At first sight, this could be interpreted as a dominant aromatic domain in the humic acid macromolecules, probably related to the climatic conditions and intense biogeochemical activity on the site under study.

A detailed inspection of the visible spectra (Fig. 4), however, suggested some weak shoulders in some of the samples, which were clearly resolved in the 2nd derivative spectra, showing valleys of variable intensity at *ca.* 465, 530, 570 and 620 nm. This coincides with the pattern reported by Kumada and Hurst (Kumada, 1967) for the soil pigments (*Pg* fractions) referred to as 'green humic acids', which consist of fungal products containing perylenequinonic pigments generated during the synthesis of hydroxynaphthalene-derived melanins (Almendros et al., 1985, Bell and Wheeler, 1986, Valmaseda et al., 1989). The occurrence of these spectroscopic maxima, not systematically present in all types of humic acids, is not unusual (Oyonarte et al., 1994; Almendros et al., 2005) and in this case could also represent a valid surrogate biomarker of fungal activity playing a role in the accumulation of stable C forms in soil.

3.4. Spectroscopic studies: Infrared spectroscopy

The alkyl skeletal structures of humic acids, reflected by the medium-to-high intensity bands at 2920, 1460, 1370 and *ca.* 720 $cm^{-1,}$ and the aryl structures, ill-resolved peaks where aromatic vibrations contribute to peaks at *ca.* 1510 cm^{-1} and 1620 cm^{-1}, were apparent in the resolution-enhanced spectra, their intensity being measured in full-scale normalized spectra (Table 5).

Concerning oxygen-containing functional groups, all spectra showed the unspecific 3400 cm^{-1} stretching band for H-bonded O–H groups, the well-defined carboxyl band at 1720 cm^{-1} and, in the resolution-enhanced spectra, a band near 1775 cm^{-1} which could correspond to oxygen in esters or heterocyclic structures. Some spectra show broad amide bands (at *ca.* 1660, 1535 cm^{-1}) although some contribution of carboxyl groups conjugated to aromatic rings could also be considered in the former band.

A systematic feature of the resolution-enhanced spectra is a systematic band pattern consisting of peaks at 1510, 1460, 1420, 1270, 1230 and 1030 cm^{-1} which agrees with that usually described in lignins (Fengel and Wegener, 1984). In the resolution-enhanced spectra, no prominent carbohydrate pattern was noted at around 1000 cm^{-1}; the absorption in this region could correspond to methoxyl (1030 cm^{-1}) in addition to some ethers and alcoholic groups.

4. Discussion

4.1. Factors affecting the accumulation patterns of the different humic substances. Quantitative features

The analysis of the distribution of the total soil C into the different humus fractions suggested humification processes in a medium with calcium saturation favouring the insolubilization of low molecular weight precursors of fulvic and humic acids otherwise subjected to biodegradation or leaching.

In most cases humin amounted to more than half of the total soil C. No systematic differences between absolute concentrations were found when considering vegetation types or soil use, but Fig. 3—where the organic fractions are calculated as percentages of the total C and the resulting bar diagrams are ranked by elevation—, could illustrate the impact of climatic range and use of the soils. In soils developed at the highest elevation, mainly occupied by climax pine forest or herbaceous vegetation (soil samples 9, 10, 20...), the accumulation of humic acids is not especially favoured, the humic acid concentration being similar to that of fulvic acids directly extracted at acid pH. To a large extent, carbon accumulation patterns at these sites are produced by the retention of humic

substances of a low molecular weight. Increased accumulation of extractable humic fractions and the humic acid-to-fulvic acid ratio close to the unity—was found in the intermediate range of the altitudinal series (e.g., samples 2 and 3) and could be attributed to the ameliorant character traditionally ascribed to deciduous Mediterranean sclerophylic vegetation, either oak forest or bush formations. Finally, soil organic matter from soil samples collected at a lower elevation (soils 15, 19…) showed—compared to the above soils—an intermediate composition: these soils accumulate non-decomposed plant residues (light fraction) and a lower amount of humic acids compared with fulvic acids and humin.

4.2. Spectroscopic data potential to establish the origins of humus variation

A rapid inspection of the spectroscopic data in the visible range indicates a conspicuous trend consisting of the fact that the higher the optical density was, the higher the intensity of the perylenequinonic bands (Fig. 4). This point to the occurrence of humification mechanisms leading to the maturation of humic acids (*i.e.*, increase of aromaticity and degree of condensation) at the expenses of intense biogeochemical activity responsible for the accumulation of microbially-reworked humic acids accompanied by microbial metabolites. In fact, a simple regression analysis showed a very significant ($P < 0.01$) correlation between the E_4 and the intensity of the valley at 570 nm in the second derivative spectra.

When comparing the resolution-enhanced infrared spectra of the different humic acids (Fig. 5), it was observed that the "lignin pattern" was more or less evident in the samples, pointing to a variable accumulation of such plant macromolecule as a major humification mechanism in these conditions (Kögel et al., 1988). A visual inspection of the

spectra was used as a criterion to establish a continuous ranking between those broadband spectra where the lignin pattern was largely smoothed out (e.g., samples 4, 16...) and the spectra where not only lignin, but protein bands (1660, 1550 cm^{-1}) were resolved. In the latter samples, other low intensity bands were also typical for lignins (at 1270, 1230 cm^{-1} methoxyphenolic vibrations for vanillyl and siryngyl groups, at 1130 cm^{-1} syringyl vibration, or at 1030 cm^{-1} peak for methoxyl groups). Parenthetically, in these complex IR spectra, it could also be noted that the 1130 cm^{-1} peak is of lower intensity in humic acids from pine vegetation soils, as expected from the guayacyl-type lignin in gymnosperms (Fengel and Wegener, 1984), whereas its intensity was high in humic acids of soils developed under angiosperms plants.

The result of this ranking of the spectra is illustrated in Fig. 5 where the resolution-enhanced spectra are classified (top to bottom) according to the apparent selective preservation of lignin structures in the humic acids. For statistical data treatments, this rank (IR_Lig_Patt, Fig. 7) was used as an additional index presumably informing on the extent of the diagenetic transformation of plant macromolecules vs. alternative condensation processes of soil compounds (Spielvogel, et al., 2004).

In fact, when the E_4 optical density obtained by visible spectroscopy is examined in comparison with the infrared spectra (Fig. 5) a clear trend towards a darker colour was observed in those humic acids with less defined lignin (the correlation between E_4 and this semiquantitative lignin alteration index was highly significant, $P< 0.01$) indicating that optical density of the humic acid in the site study could inform on the extent to which they are not formed by structural rearrangement of plant lignins.

358 *4.3. Assessment of factors related with the soil carbon levels*

359

360 In order to analyze the factors with a probable bearing on the C sequestration in
361 the scenario under study, multiple regression models and multidimensional scaling
362 (Kruskal, 1964) were used. Compared with the principal component analysis, the latter
363 non-linear mapping procedure forces to illustrate the whole information described by the
364 original variables into an *n*-dimensional (e.g., *n*=2) space, avoiding a supervised selection
365 of factorial axes explaining only a portion of the total inertia (Fig. 6). The iterative
366 algorithm leading to a final arrangement of the points representing the variables
367 converges on a configuration where the differences between the values of the
368 classification index (in this case squared Euclidean distances) and the distances in the
369 space is minimum. This is unavoidably associated with a distortion of the monotony of
370 the distances in the plots (Eshuis et al., 1977), their extent being reflected by the
371 parameter referred to as stress (in this case 0.077, suggesting reliability of the two-
372 dimensional representation). This procedure was selected because it does not require
373 making statistical assumptions on the distribution of data. In fact, our previous supervised
374 detailed inspection of the regression plots between variables in several cases suggested a
375 non-linear relationship (Fig. 2).

376 Multidimensional scaling was here used as a possible tool to help isolate relevant
377 variables from being further considered in multiple regression models to quantify
378 significant environmental factors connected with the accumulation of oxidizable C in
379 soil. The plot shown in Fig. 6 suggested independent variables to a different extent
380 associated with C concentration in the topsoil. Those encircled are positively correlated
381 with the C concentration, and those into the innermost circle (Slope, SLF) were those
382 remaining in the multiple regression models independently calculated by using the

automatic backwards selection of the variables (C= 0.304*Slope - 0.057*SLF). The remaining dependent variables were automatically rejected (or removed under supervision) from the model due to colinearity effects or their poor (P>0.05) contribution to the total variance of the model. As a whole, this plot suggested a significant role of local factors in the accumulation of C (topographical and lithological). It points to preferential C accumulation favoured by water retention and the transportation of sedimentary organic matter and fine soil mineral fractions. On the other hand, it is possible that intense solar irradiation and carbonates in the microenvironments with a more pronounced semiarid character might be playing a role in the organic matter biodegradation.

4.4. Factors controlling the humification pathways in the site under study

Several multivariate data treatments were used to investigate the humification processes on the site studied. In particular, cluster analysis, analysis of variance and discriminant analysis (not shown) led us to consider that vegetation had little or no significant effect on soil quality. By using the discriminant analysis, we examined several classification factors consisting of types of vegetation (taxonomical or ecophysiological differences) as well as forest age and soil use, but no model was obtained displaying clear patterns attributable to any of the above independent variables. Consequently, the following strategies were focused on exploring the utility of chemical descriptors in identifying variable patterns defining the possible independent origin of soil organic matter.

A principal component analysis (Fig. 7) clearly showed two clusters of samples defined by different quality descriptors. It also showed the above-indicated fact that the

types of vegetation were not responsible for pattern formation. Samples "a priori" characterized by low environmental quality (e.g., 10, 9, 3, 14... consisting of old forest formations with raw humus or secondary brushwoods) showed comparatively high C levels. This accumulation of raw C forms in soils of comparatively high C-to-N ratios (associated with high intensity of the IR 2920 cm^{-1} band, marked lignin patterns in the IR spectra) suggests slightly altered macromolecules in the HA fraction, the accumulation of which was probably due to C stabilization processes favoured by local and microtopographical constraints (e.g., SLF, W and clay, Fig. 7) suggesting that the accumulation of water and fine soil particles might be favoured biomass production and preservation at these sites. With some criterion, the positive soil properties at these sites depended on the organic matter quantity, not its quality: the soils have a high CEC but when these variables were processed as rates (CEC-to-C) the directions of the eigenvectors turn, as expected, towards the second cluster (samples 18, 13, 8, 1...) including young forests formations as well as cultured sites. In this second cluster of samples, the loading factors suggested a high biogeochemical organic matter transformation: The HAs show high aromaticity and microbial quinoid pigments. The role of carbonates and higher pHs at these sites should not be discarded as factors favouring mineralization processes and organic matter maturity. In addition, the values for total solar radiation and sunlight hours (RGS_V, HS_V) could be associated with strong seasonal moisture changes typical of the continental Mediterranean climate which is considered to favour the formation and maturation of humic acids.

4.5. Conclusions

The results obtained indicate the possibility of identifying the local impact of soil use and management by taking advantage of suitable biogeochemical descriptors, mainly consisting of humic acids spectroscopic characteristics. In fact, some soils (such as those of ancient forests and soils at the upper areas of the altitudinal gradient) present favourable physical and biogeochemical properties as a consequence of the high concentration of organic matter with a low degree of humification. These humus formations consist mainly of fulvic and humic acids with a strong aliphatic character and low molecular weight, to all appearances formed by a progressive transformation of plant lignins in relatively undisturbed humus types of comparatively low biological activity (Cerli et al., 2006).

This pattern contrasts with that found of the soils with a lower amount of organic matter, the characteristics of which (high aromaticity, complex and disordered structure) are often considered to be indicative of a high potential to maintain their properties against changes in the biogeochemical system (Almendros and Dorado, 1999). This situation tends to concur mainly in semiarid Mediterranean-type formations and very ancient pine forests.

From a practical viewpoint, soil use and management practices in the whole ecosystem have converged on two qualitative situations: A set of soils (mainly developed under ancient forests) shows valuable agro-biological quality exclusively due to high C levels of inherited humic matter from the diagenetic transformation of plant material. On the other hand, soils developed on cleared and recently reafforested plots show lower C levels, but a high degree of humification, and would presumably behave as comparatively resilient irrespective of soil use and environmental change.

Acknowledgement

The authors wish to thank the manager and personnel of the Sierra María-Los Vélez Natural Park for their help during field sampling campaigns, the Spanish CICyT for research projects CGL2004-02282BTE and BOS2002-03741, and to the Ministry of Education and Science, Spain, for the following fellowships (AP2001-3281, AP2002-3626).

References

Almendros G., Dorado J. 1999. Molecular characteristics related to the biodegradability of humic acid preparations. Structural factors related to the biodegradability of laboratory-modified humic acid preparations. Europen Journal of Soil Science 50, 227–236.

Almendros, G., Martínez, A.T., Dorado, E. 1985. Production of brown and green humic-like substances by *Ulocladium atrum*. Soil Biology and Biochemistry, 17, 257–259.

Almendros, G., Sanz, J., 1992. A structural study of alkyl polymers in soil after perborate degradation of humin. Geoderma 53, 79–95.

Almendros, G., Zancada, M.C., Pardo, M.T., 2005. Land use and soil carbon accumulation patterns in South African savanna ecosystems. Biology and Fertility of Soils 41, 173–181.

Bell, A.A., Wheeler, M.H., 1986. Biosynthesis and functions of fungal melanins. Annual Review of Phytopathology 24, 411–451.

Cerli, C., Celi, L, Johansson, M.-B, Kögel-Knabner, I., Rosenqvist, L., Zanini, E., 2006. Soil organic matter changes in a spruce chronosequence on Swedish former agricultural soil: I. Carbon and lignin dynamics Soil Science 171, 11, 837–849

CIE., 1986. Colorimetry. 2nd. Ed. CIE Central Bureau, Viena, Austria, 83 pp.

CSIC., 1969. Métodos analíticos de la Estación Experimental del Zaidín. CSIC. Granada.

Cueto, M., Blanca, G., 1997. Flora del Parque Natural de Sierra María-Los Vélez. Sociedad Almeriense de Historia Natural, Almería.

Dabin, B., 1971. Étude d'une méthode d'extraction de la matière humique du sol. Science du Sol 2, 15–24.

Derenne S., Knicker H. 2000. Chemical structure and preservation processes of organic matter in soils and sediments Organic Geochemistry 31, 7–8, 2000, 607-608

Duchaufour, P., 1977. Pédogenèse et Classification. Pédologie, 1. Masson, Paris.

Duchaufour, P., Jacquin, F., 1975. Comparaison des processus d'humification dans les principaux types d'humus forestiers. Bulletin de l'Association Française pour l'Étude du Sol 1, 29–36.

Egea, D., 1986. Geología de la zona centro-oriental de las Cordilleras Béticas (Comarca de los Vélez, Almería). Síntesis bibliográfica. Revista Velezana 5, 89–120.

Eshuis, W., Kistemaker, P.G., Meuzelaar, H.L.C., 1977. Some numerical aspects of reproducibility and specificity. In: Analytical Pyrolysis, pp. 151–166 (eds Jones, C.E.R. & Cramers, C.A.). Elsevier, Amsterdam.

Fengel, D., Wegener, G., 1984. Wood: Chemistry, Ultrastructure, Reactions. Walter de Gruyter, Berlin.

Holgrem, G.S., 1967. A rapid citrate-dithionite extractable iron procedure. Soil Science Society of America Proceedings 31, 210–211.

507 Institut Technique des Céréales et des Fourrages (ITCF)., 1988. STAT-ITCF. Manuel
508 d'Utilisation. Atelier, Paris.
509 Kögel I., Ziegler F., Zech W., 1988. Lignin signature of subalpine Rendzinas (Tangel-
510 and Moderrendzina) in the Bavarian Alps. Zeitscrift für Pflanzenernährung
511 Bodenkunde 151, 15-20.
512 Kögel-Knabner, I., Lützow, M.V., Guggenberger G., Flessa, H., Marschner B., Matzner
513 E., Ekschmitt, K., 2005, Mechanisms and regulation of organic matter stabilisation in
514 soils (Editorial). Geoderma 128, 1–2.
515 Kononova, M.M., 1961. Soil Organic Matter. Pergamon, New York.
516 Kruskal, J.B., 1964. Multidimensional scaling by optimising goodness of fit to a
517 nonmetric hypothesis. Psichometrika 29, 1–27.
518 Kumada, K., Hurst, H.M., 1967. Green humic acid and its possible origin as a fungal
519 metabolite. Nature 214, 631–633.
520 Miralles, I., Ortega, R., Cantón, Y., Asensio, C., 2002. Degradación del suelo por exceso
521 de sales y su relación con la topografía en un área del sur de España. Agrochimica 46,
522 270–279.
523 Moore, I.D., Grayson, R.B., Ladson, A.R., 1991. Digital terrain modelling: a review of
524 hydrological, geomorphological and biological applications. Hydrological Processes
525 5, 3–30.
526 Nelson, D.V., Sommers, L.E., 1982. Total carbon, organic carbon and organic matter. In:
527 Methods of Soil Analysis: Part 2, Chemical and Microbiological Properties, 2nd edn.
528 pp. 539–579 (eds Page, A.L., Miller, R.H., Keeney, D.R.), American Society of
529 Agronomy, Madison, WI.

530 Orlóci, L., Kenkel, N.C., 1985. Introduction to Data Analysis, with Examples from
531 Population and Community Ecology. International Cooperative Publishing House,
532 Fairland, Md.
533 Oyonarte, C., Pérez-Pujalte, A., Delgado, G., Delgado, R., Almendros, G., 1994. Factors
534 affecting soil organic matter turnover in Mediterranean ecosystems from Sierra de
535 Gador (Spain): an analytical approach. Communications in Soil Science and Plant
536 Analysis 25, 1929–1945.
537 Richards, L.A., 1954. Diagnosis and Improvement of Saline and Alkali Soils. Handbook,
538 60. V. S. Salinity Laboratory, U.S. Department of Agriculture.
539 Rivas Martínez, S., 1987. Memoria del Mapa de Series de Vegetación de España
540 1:400.000. ICONA, Madrid.
541 Rosenfeld, A., Kak, A.C., 1982. Digital Picture Processing, 1. Academic Press, New
542 York.
543 Savage, S.M., Osborn, J., Letey, J., Heaton, C., 1972. Substances contributing to fire-
544 induced water repellency in soil. Soil Science Society of America Proceedings 36,
545 674–678.
546 Schulze, D.G.J., Ángel, L., Van Scoyoc, G.E., Henderson, T.L., Baumgardner M.F., Stott
547 D.E., 1993. The significance of organic matter in determining soil color. pp. 71-90.
548 In: Soil Color. Soil Science Society of America Special Publication No 31, (eds
549 Bigham, J.M., Ciolkosz, E.J.). Soil Science Society of America, Madison, WI.
550 Soil Conservation Service, 1984. Soil Survey Laboratory Methods and Procedure for
551 Collecting soil Samples. Soil Survey investigations, Report No 1 (Revised 1984), U.S.
552 Department of Agriculture, Washington, D.C.
553 Spielvogel, S., Knicker, H., Kogel-Knabner I., 2004. Soil organic matter composition and
554 soil lightness. Journal of Plant Nutrition and Soil Science 167, 545–555.

555 Traina, S.J., Novak, J., Smeck, N.E., 1990. An ultraviolet absorbance method of
556 estimating the percent aromatic carbon content of humic acids. Journal of
557 Environmental Quality 19, 151–153.
558 Valmaseda, M., Martínez, A.T., Almendros, G. 1989. Contribution by pigmented fungi
559 to P-type humic acid formation in two forest soils. Soil Biology and Biochemistry, 21,
560 23–28.
561

Table 1
General characteristics of the samples under study

Sample label	Longitude[b]	Latitude[b]	Geological substrate	Horizon depth / cm	Elevation / m	Slope / %	Vegetation	Soil type
1	580061	4169248	Detritic limestone material	Ah (0–12)	1053	16	Reafforested pine forest (*Pinus halepensis*)	Mollic Petric Calcisol
2	575266	4168224	Clastic limestone material	Ah (0–8/13)	1141	17	Cleared bush encroached site (*Stipa tenacissima, Lygeum spartum, Genista scorpius, Artemisia* sp.)	Rendzic Leptosol
3	569731	4172029	Detritic limestones and marls	Ah (0–11)	1398	45	Relictual oak forests (*Quercus ilex* ssp. *rotundifolia*)	Hypocalcic Calcisol
4	579112	4169374	Detritic limestones	Ah (4–22)	1231	25	Reafforested pine Forest (*Pinus halepensis*)	Hypercalcic Calcisol
5	572910	4173545	Calcareous conglomerates	Ap (0–18)	1230	11	Orchard (almond trees)	Hypocalcic Luvic Calcisol
6	567162	4173221	Clastic limestones	Ah (0–29)	1140	13	Climatic pine forest (Pinus halepensis)	Hypercalcic Calcisol
7	564687	4173383	Detritic sediments	Ap1 (0–14)	1089	9	Cereal cultivated-site	Hypercalcic Petric Calcisol
8	578314	4173493	Marls and limestones	Ah (0–20)	1123	19	Reafforested pine forest (*Pinus halepensis*)	Petric Calcisol
9	568868	4170037	Detritic limestones	Ah1 (5–20)	1600	61	Climax pine forest (*Pinus nigra*)	Calcic Chernozem
10	568865	4170153	Detritic limestones and dolomies	Ah (10–32)	1520	40	Climax pine forest (*Pinus nigra*)	Calcic Chernozem
11	576675	4180401	Limestones	Ah (0–14)	1508	18	Alpine brush (*Juniperus oxycedrus, Vella spinosa, Erinacea antillis, Quercus coccifera*)	Calcaric Rendzic Leptosol
12	578049	4177831	Alluvial calcic marls	Ah1 (0–22)	1024	7	Orchard (almond trees)	Gleyc Hypocalcic Calcisol
13	581257	4182563	Marls and limestones	Ah (0–14)	899	16	Reafforested pine forest (*Pinus halepensis*)	Hypercalcic Calcisol
14	586814	4178805	Limestones	Ah1 (0–10)	1122	33	Relictual oak forests (*Quercus ilex* ssp. *rotundifolia*)	Mollic Calcaric Cambisol
15	585631	4184450	Limestones	Ah (0–20)	892	25	Chaparral-like brushlands (*Quercus ilex* ssp. *rotundifolia* and *Juniperus phoenicia*)	Hypercalcic Petric Calcisol
16	587608	4176042	Limestones	Ah (0–13/27)	1412	15	Chaparral-like brushlands (*Quercus ilex* ssp. *rotundifolia* and *Juniperus phoenicea*)	Calcaric Rendzic Leptosol
17	587132	4177350	Limestones	Ap (0–20)	1113	12	Cereal cultivated-site	Hypercalcic Calcisol
18	582951	4176462	Marls and limestones	Ap (0–20)	900	9	Orchard (almond trees)	Anthropic Calcaric Regosol
19	584190	4176434	Detritic limestone material	Ah1 (2–4)	988	38	Climax pine forest (*Pinus halepensis*)	Mollic Calcaric Cambisol
20	571380	4170390	Limestones	Ah (0–12/15)	2043	2	Alpine brush (*Vella spinosa, Erinacea antillis*, *Lygeum spartum*)	Calcaric Rendzic Leptosol

[b] Universal Transverse Mercator

Table 2

General topographical features of the sites under study calculated with a geographical information system

Sample label	W	SLF	R	Ct	CI	Gsr Summ Sols	Gsr Win Sols	Gsr Equ	Sun h Summ Sols	Sun h Win Sols	Sun h Equ
1	8.5	3.8	1	-0.0025	0.0025	8010	1908	5189	12	9	11
2	8.4	5.4	1	-0.0024	0.0001	8142	2063	5392	12	9	11
3	10.5	87.9	30	0.0055	-0.0045	7689	1098	4185	13	4	10
4	7.0	24.3	1	-0.0046	-0.0021	7767	2456	5677	12	8	10
5	11.3	5.3	10	0.0000	0.0000	8145	1747	5040	14	7	11
6	8.0	23.8	2	0.0006	-0.0069	7845	2079	5292	12	8	10
7	9.6	5.9	3	0.0025	-0.0025	8045	1687	4937	14	8	11
8	8.5	13.2	2	0.0015	0.0040	7950	1491	4702	13	6	10
9	9.3	122.6	14	0.0047	-0.0053	7028	622	3196	13	0	9
10	10.0	139.8	29	0.0000	0.0100	7258	635	3426	13	0	9
11	19.2	3.4	1	0.0000	0.0000	8372	1942	5320	14	9	11
12	8.0	7.0	1	-0.0025	0.0025	7920	1510	4695	14	8	10
13	8.8	39.1	5	-0.0008	0.0033	7503	1271	4271	13	6	10
14	10.0	80.8	20	0.0062	0.0012	7437	1000	3907	12	5	8
15	7.9	8.8	1	-0.0010	0.0061	7840	1784	4986	13	8	10
16	7.5	13.6	1	-0.0041	0.0009	8223	2318	5683	14	9	11
17	10.1	23.2	10	0.0000	0.0000	7924	1443	4641	14	6	11
18	9.8	11.3	5	-0.0005	-0.0005	7864	1656	4860	13	7	10
19	7.9	8.8	1	-0.0084	0.0040	7830	1807	5017	12	7	10
20	7.7	34.4	2	-0.0055	0.0020	8334	2801	6189	13	9	11

W: wetness index, SLF: Slope length factor, R: contributing area, Ct: slope plan curvature, CI: slope profile curvature, Gsr Summ Sols: global solar radiation at summer solstice, Gsr Win Sols: global solar radiation at winter solstice, Gsr Equ: global solar radiation at equinox, Sun h Summ Sols: hours of insolation at summer solstice, Sun h Win Sols: hours of insolation at winter solstice, Sun h Equ: hours of insolation at equinox.

Table 3

General analytical characteristics of the soil samples

		1	2	3	4	5	6	7	8	9	10	11	12	13	14	15	16	17	18	19	20
Total sand (2–0.02 mm)	(g kg^{-1})	502	391	327	597	310	414	572	513	257	344	110	69	423	74	161	64	331	160	508	203
Total silt (0.02–0.002 mm)	(g kg^{-1})	273	372	276	214	311	294	256	378.	471	332	399	263	379	372	364	420	376	456	182	315
Total clay (<0.002 mm)	(g kg^{-1})	225	237	397	189	379	292	173	108	272	324	490	668	198	554	475	516	293	384	309	482
water holding capacity	(g cm^{-3})	154	140	283	117	178	193	118	59	341.	267	412	209	91	252	290	325	161	139	521	238
Bulk density	(g cm^{-3})	1.2	1.3	0.8	1.3	1.0	0.7	1.2	1.3	1.1	1.1	1.3	1.1	1.0	0.7	0.5	1.1	1.0	1.1	0.9	1.3
pH (H_2O)		7.8	8.3	7.7	8.0	8.5	8.2	8.5	8.4	7.9	8.1	7.7	8.3	8.4	7.6	8.0	7.9	8.2	8.5	7.3	7.9
$CaCO_3$	(g kg^{-1})	576	528	278	673	175	313	588	940	360	544	46	439	803	5	294	42	674	703	248	380
Soil C	(g kg^{-1})	23.2	18.6	81.2	31.3	14.5	32.2	13.2	13.2	85.4	74.4	107.4	6.9	19.0	50.3	49.0	52.9	23.4	5.9	195.3	25.0
Soil N	(g kg^{-1})	1.5	1.6	4.3	2.3	1.3	2.0	1.1	0.8	2.9	2.0	10.4	0.9	0.7	3.5	3.6	6.6	2.4	0.2	12.9	6.4
C-to-N ratio		15.9	11.5	18.8	13.9	11.4	16.1	12.4	16.0	29.8	37.7	10.3	8.1	25.9	14.3	13.5	8.0	9.7	26.2	15.1	3.9
CEC	($cmol_c$ kg^{-}	21.9	21.5	41.9	25.0	27.2	30.7	12.7	9.2	53.9	7.9	50.4	24.8	10.7	37.6	35.9	37.1	17.1	8.2	46.2	26.9
Exchangeable K	($cmol_c$ kg^{-}	0.4	0.3	2.0	0.2	1.5	0.8	0.5	0.2	0.3	1.0	3.1	0.6	0.2	1.1	0.3	1.1	0.4	0.3	1.2	1.8
Exchangeable Ca	($cmol_c$ kg^{-}	19.9	19	36.6	22.9	23.3	23.4	10.6	6.6	43.3	4.7	44.6	19.5	10	35	34.9	35.1	16.2	6.2	41.4	24.3
Exchangeable Mg	($cmol_c$ kg^{-}	1.6	2.2	3.3	1.9	2.4	6.5	1.6	2.4	10.3	2.2	2.7	4.7	0.5	1.5	0.7	0.9	0.5	1.7	3.6	0.8
Free Fe	(mg kg^{-1})	5.3	8.8	5.8	2.1	8.6	8.7	3.5	2.0	5.8	4.0	23.6	1.0	1.0	24.5	6.8	27.8	5.6	1.7	3.4	2.6
WDPT class		Sl	Nr	Se	Nr	Nr	Nr	Nr	Nr	Sl	Sl	Sl	Nr	Nr	Nr	Nr	Nr	Nr	Nr	St	Nr
CIELAB L*		47.3	39.2	29.8	39.6	40.3	36.2	53.2	50.2	34.0	33.9	29.8	59.8	65.1	35.3	39.2	31.5	51.1	77.9	36.9	38.3
CIELAB C_{ab}*		17.0	18.6	12.4	11.9	21.9	13.9	14.9	20.1	11.2	11.1	13.2	10.2	16.4	21.6	11.6	14.1	15.5	11.2	13.6	16.8
CIELAB H_{ab}		68.1	65.8	63.7	67.7	61.2	65.9	70.9	68.3	68.6	69.6	63.8	80.2	77.7	57.8	66.9	62.2	71.0	81.3	66.1	68.1

Sample labels refer to the Material and methods section

Db= Bulk density, CEC= cation exchange capacity, WDPT (water drop penetration time) classes: Nr-Nonrepellent (< 5 sec), Sl: slight (10-60 sec), St: Strong (180–600 sec), Se: Severe (900-3600 sec).

Table 4

Total soil carbon distribution into the different organic fractions

Sample label	Light fraction	Total humic extract	Humic acid (HA)	Fulvic acid (H_3PO_4-extracted)	Fulvic acid (NaOH–extracted) (FA)	Non-extractable humin	HA-to-FA
	(C g ·100 g soil^{-1})						
2	0.02	1.44	0.67	0.36	0.76	1.34	0.882
3	0.23	4.67	2.07	0.55	2.59	2.67	0.800
5	0.08	0.50	0.23	0.14	0.27	1.04	0.833
9	0.14	4.03	0.86	0.49	3.17	3.89	0.271
10	0.07	2.80	0.72	0.66	2.08	3.28	0.345
15	0.21	2.51	0.74	0.41	1.77	2.95	0.418
19	0.78	7.11	2.63	1.02	4.48	10.62	0.587
20	0.06	1.44	0.29	0.29	1.14	2.17	0.255

Table 5

Spectroscopic data of humic acids

		Intensity of the valleys (wavelength nm^{-1}) in the second derivative spectrum (absorption units)		Optical density values of the main bands (wavelength cm^{-1}) in the infrared spectra (absorption units)						
Sample label	E_4	620	570	3400	2920	1720	1620	1510	1530	S-to-G
1	0.70	0.0020	0.0007	0.617	0.533	0.628	0.739	0.429	0.495	0.84
2	1.23	0.0024	0.0011	0.500	0.478	0.704	0.709	0.410	0.476	0.69
3	0.56	0.0016	0.0006	0.711	0.528	0.636	0.697	0.376	0.430	0.82
4	1.16	0.0027	0.0012	0.496	0.441	0.665	0.655	0.367	0.437	0.69
5	0.66	0.0018	0.0006	0.619	0.543	0.677	0.793	0.455	0.524	0.83
6	0.71	0.0019	0.0007	0.612	0.489	0.602	0.717	0.417	0.501	0.76
7	0.97	0.0018	0.0008	0.597	0.500	0.635	0.681	0.423	0.461	0.84
8	0.63	0.0021	0.0007	0.700	0.577	0.702	0.754	0.459	0.509	0.79
9	0.86	0.0020	0.0008	0.686	0.505	0.591	0.646	0.368	0.406	0.79
10	0.73	0.0019	0.0007	0.669	0.569	0.646	0.684	0.408	0.449	0.79
11	0.84	0.0020	0.0007	0.611	0.514	0.625	0.680	0.414	0.465	0.73
12	1.26	0.0020	0.0009	0.593	0.492	0.708	0.710	0.386	0.509	0.66
13	0.59	0.0018	0.0010	0.651	0.442	0.567	0.706	0.402	0.454	0.80
14	0.62	0.0009	0.0004	0.689	0.555	0.615	0.726	0.417	0.482	0.78
15	0.95	0.0021	0.0008	0.625	0.488	0.684	0.700	0.386	0.456	0.72
16	1.10	0.0019	0.0011	0.691	0.455	0.615	0.726	0.434	0.482	0.66
17	0.87	0.0021	0.0009	0.618	0.527	0.683	0.725	0.456	0.500	0.74
18	0.30	0.0013	0.0003	0.746	0.492	0.592	0.788	0.434	0.468	1.06
19	0.52	0.0015	0.0004	0.726	0.584	0.680	0.699	0.389	0.403	0.83
20	0.64	0.0028	0.0011	0.646	0.578	0.672	0.767	0.486	0.522	0.87

562

563 **Figure captions**

564

565 Fig. 1. Location map of the studied sites in the Natural Park Sierra María-Los Vélez
566 Natural Park.

567 Fig. 2. Relationships between CIELAB L* (a colour descriptor of the whole soil) and the
568 organic carbon content of air-dried soils.

569 Fig. 3. Quantitative distribution of the total soil C into different organic matter fractions.
570 Samples are ranked according to elevation and labelled with types of vegetation.

571 Fig. 4. Visible spectra (right ordinate axis, a) and second derivative spectra (left ordinate
572 axis, b) of humic acids. Sample number (right bottom corner, Table 1) and E_4 (Table
573 5) are also shown.

574 Fig. 5. Detail of the 2000–700 cm^{-1} region of the resolution-enhanced infrared spectra of
575 humic acids showing progressive lignin alteration levels in the different soils. The E_4
576 optical density (Table 5) is also shown for comparison.

577 Fig. 6. Multidimensional scaling of environmental factors related to carbon concentration
578 in soils. Encircled variables present significant ($P<0.05$ coefficients in multiple
579 regression models explaining soil C accumulation in terms of the independent
580 variables shown in the plot: SLF: Slope length factor, W: Wetness index, GSR_E:
581 Global solar radiation at equinox, SH_E: Sun hours at equinox.

582 Fig. 7. Representation, in the space defined by the first two factors obtained by principal
583 component analysis, of the scores corresponding to soil samples (number codes refer
584 to Table 1), showing groups interpreted as different humification mechanisms.
585 Contribution of the original variable to the components is shown with the
586 superimposed vectors: CEC: Cation exchange capacity, IR_2920 normalized intensity

of the C-H stretching band in the IR-spectra, SLF: Slope length factor, IR_Lig_Patt: extent of the relative preservation of lignin structures suggested by infrared spectroscopy (Fig. 5), C-to-N: soil carbon-to-nitrogen ratio: an optical density ratio decreasing with the increasing molecular size, DHPQ620: intensity of the 620 nm valley in the second derivative spectra of humic acids, produced by polycyclic quinoid pigments (Fig. 4), GSR_S: Global solar radiation in summer, E_4: Optical density of humic acid (aromaticity index), SH_E: Sun hours at equinox, W: Wetness index.

Figure

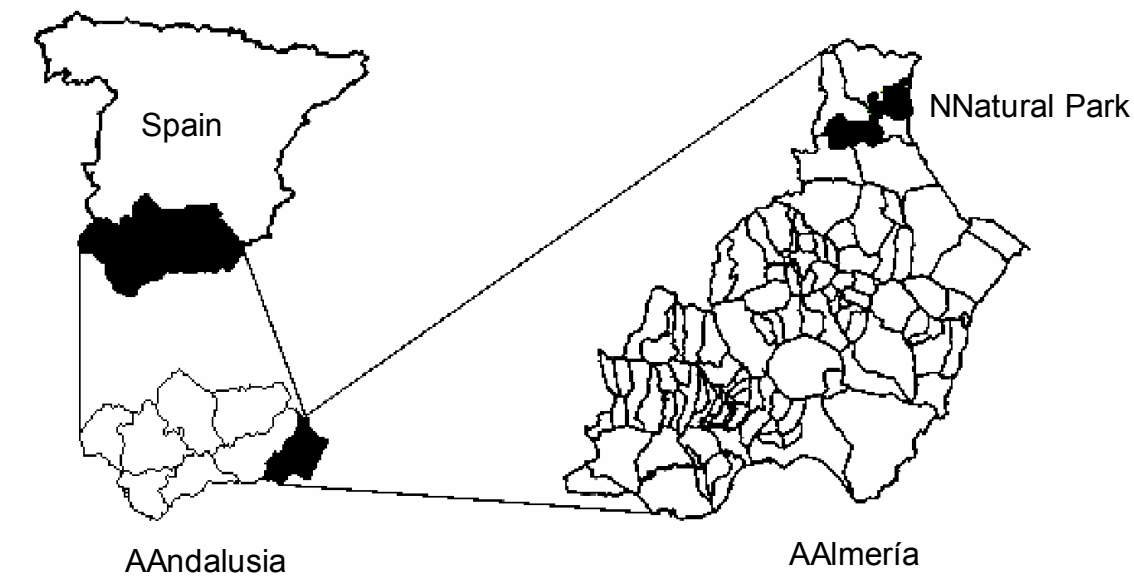

Fig 1. Location map of the studied sites in the Sierra María-Los Vélez Natural Park.

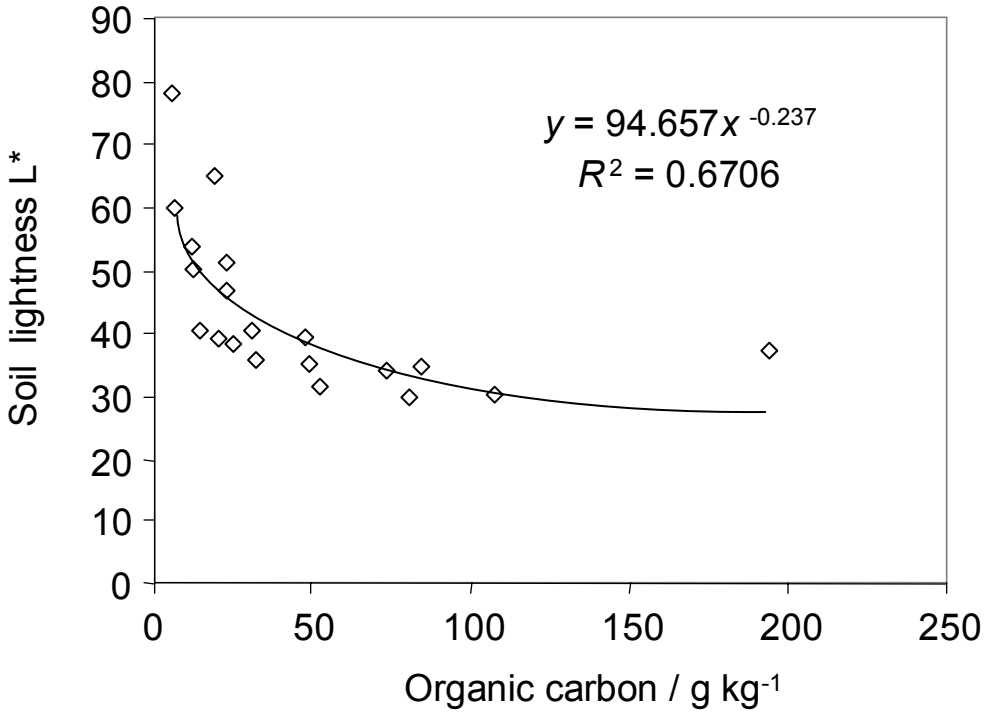

Fig. 2. Relationships between CIELAB L* (a colour descriptor of the whole soil) and the organic carbon content of air-dried soils.

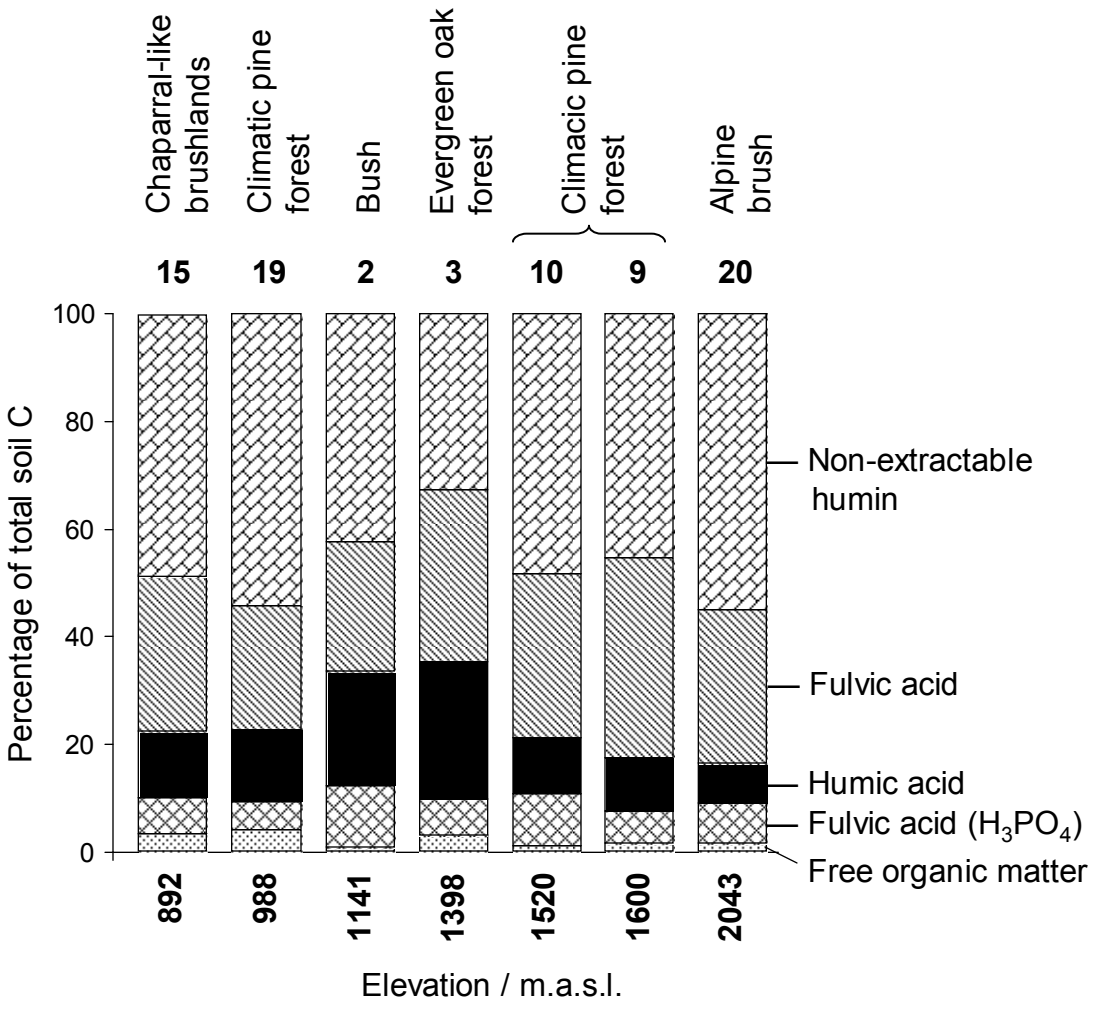

Fig. 3. Quantitative distribution of the total soil C into different organic matter fractions. Samples are ranked according to elevation and labelled with types of vegetation.

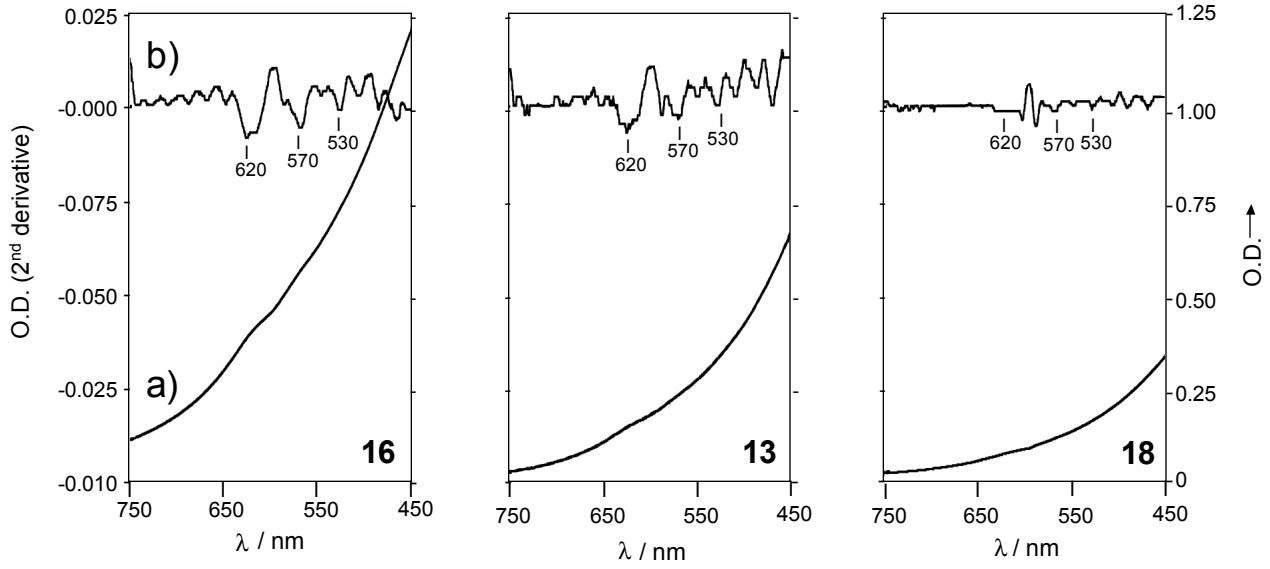

Fig. 4. Visible spectra (right ordinate axis, a) and second derivative spectra (left ordinate axis, b) of humic acids. Sample number (right bottom corner, Table 1) and E4 (Table 5) are also shown.

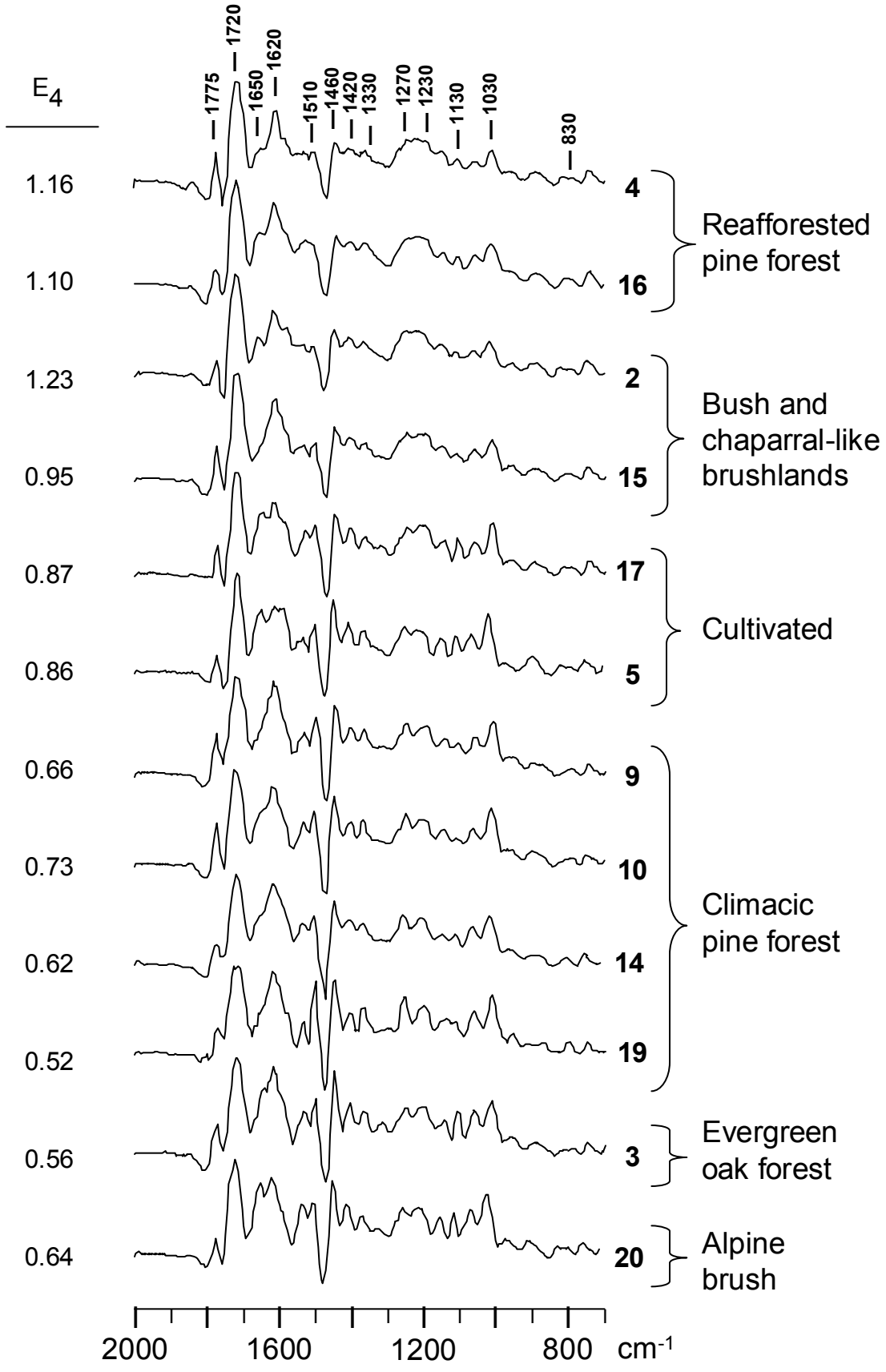

Fig. 5. Detail of the 2000–700 cm^{-1} region of the resolution-enhanced infrared spectra of humic acids showing progressive lignin alteration levels in the different soils. For comparison the E_4 optical density (Table 5) is also shown.

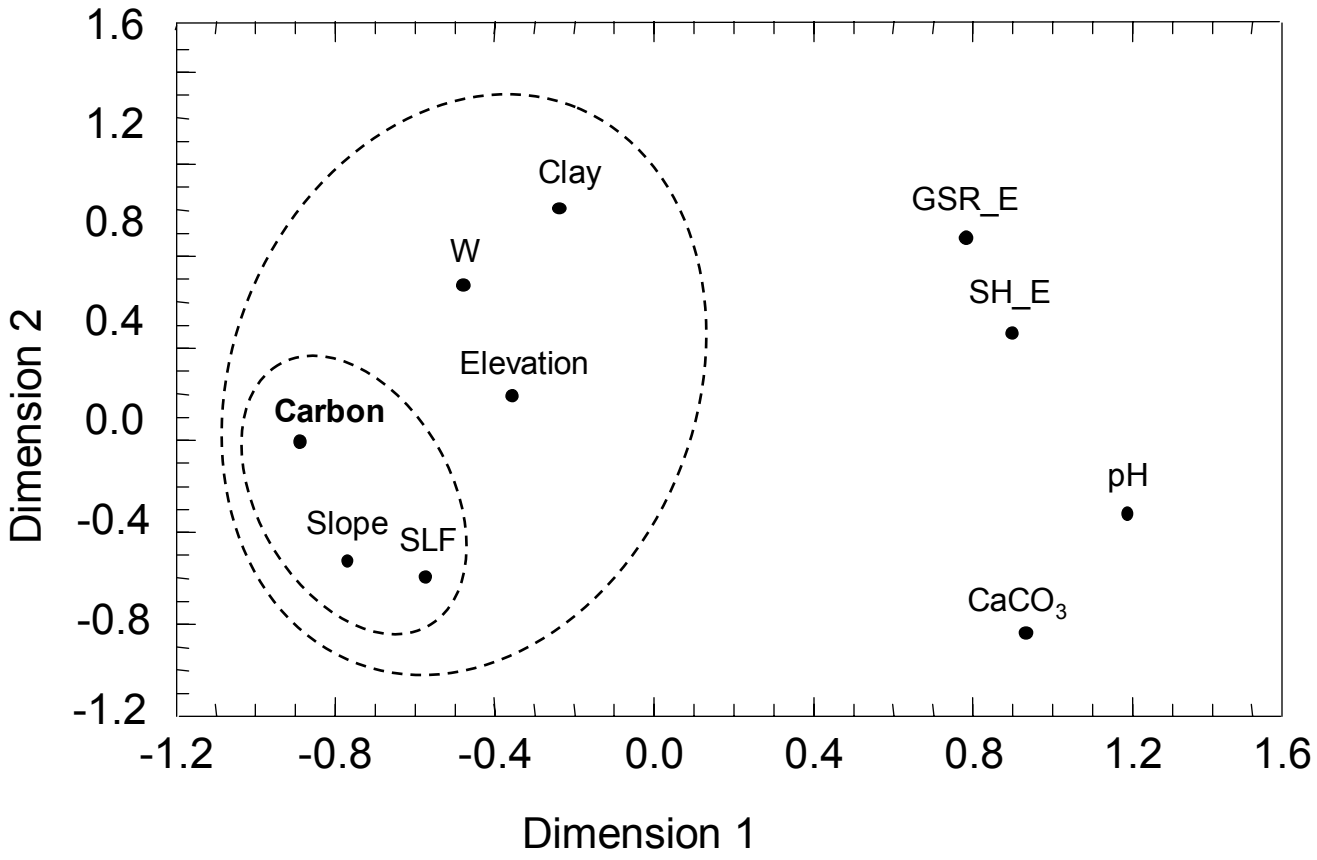

Fig. 6. Multidimensional scaling of environmental factors related to carbon concentration in soils. Encircled variables present significant (P<0.05 coefficients in multiple regression models explaining soil C accumulation in terms of the independent variables shown in the plot: SLF: Slope length factor, W: Wetness index, GSR_E: Global solar radiation at equinox, SH_E: Sun hours at equinox.

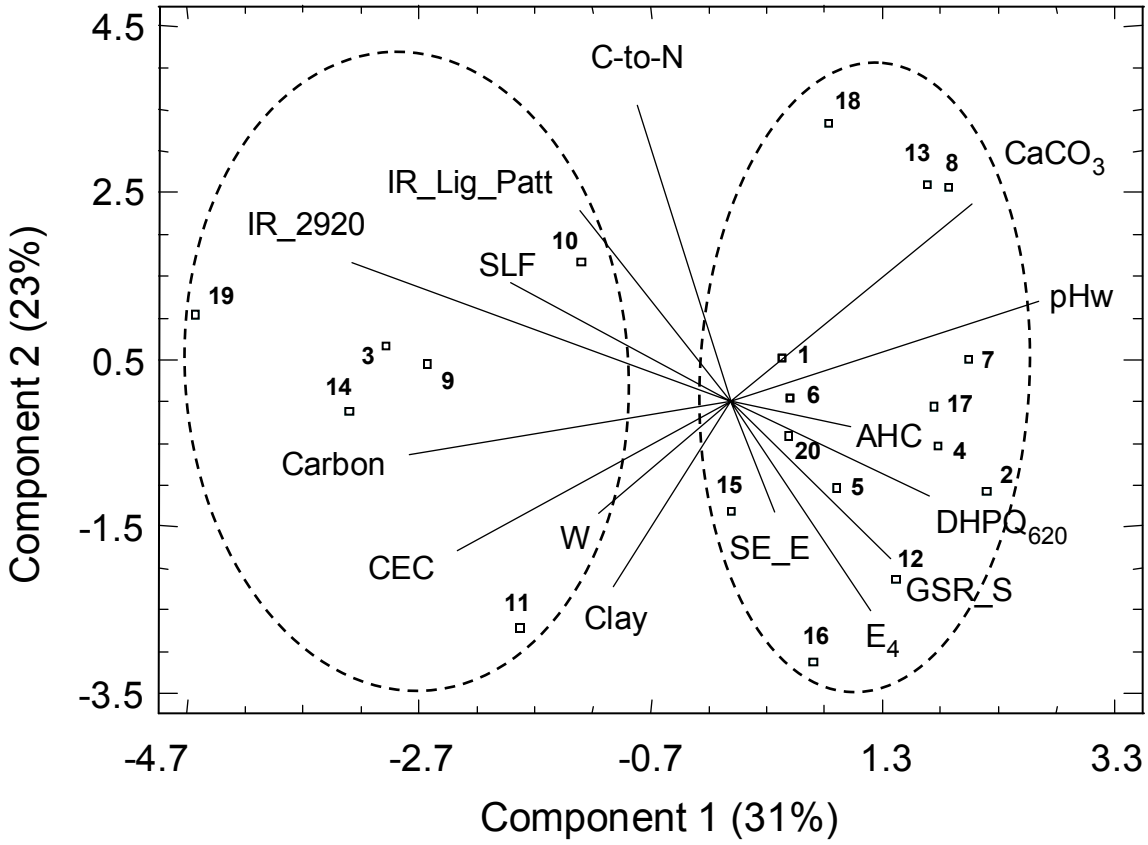

Fig. 7. Representation, in the space defined by the first two factors obtained by principal component analysis, of the scores corresponding to soil samples (number codes refer to Table 1), showing groups interpreted as different humification mechanisms. Contribution of the original variable to the components is shown with the superimposed vectors: CEC: Cation exchange capacity, IR_2920: normalized intensity of the C-H stretching band in the IR-spectra, SLF: Slope length factor, IR_Lig_Patt: extent of the relative preservation of lignin structures suggested by infrared spectroscopy (Fig. 5), C-to-N: soil carbon-to-nitrogen ratio, DHPQ620: intensity of the 620 nm valley in the second derivative spectra of humic acids, produced by polycyclic quinoid pigments (Fig. 4), GSR_S: Global solar radiation in summer, E4: Optical density of humic acid (aromaticity index), SH_E: Sun hours at equinox, W: Wetness index.